

Logic Geophysics & Analytics LLC

Draft Report

For Ground-Penetrating-Radar Surveys of the Nome Cemetery, Nome, Alaska

Date: 30 July 2018
Subject: Ground-Penetrating-Radar Surveys for the City of Nome at the Nome Cemetery, Nome, Alaska: Draft Report
To: Ms Dawn Ubelaker, Cemetery Manager, City of Nome
From: Dr. Esther Babcock, Logic Geophysics & Analytics LLC
Appendices: A: Figures; B: Anomaly Locations and Depths

Contents

1. Executive Summary	2
2. Objectives	3
3. Deliverables	3
4. Methods	3
4.1 Overview of the method	3
4.2 Equipment used	4
4.3 Survey Design.....	4
4.4 Location and Positioning	5
5. Data Quality Assurance and Quality Control (QA/QC)	5
5.2 QA/QC Tests.....	5
5.2 QA/QC Results	5
6 Project Sites	6
7. Data Analysis	7
7.1 Initial Processing	7
7.2 Plotting and Interpretation	8
8. Results	8
8.1 Interpreted burial locations and depths	8
8.2 Sources of Error and Uncertainty Analysis.....	9
9. Conclusions.....	11

1. Executive Summary

Logic Geophysics & Analytics LLC (Logic Geophysics) is pleased to submit this draft report to the City of Nome (the “City”) concerning ground-penetrating-radar (GPR) surveys at the City’s cemetery. The project objective was to collect data at 6 Areas of Concern (AOCs), then process and interpret the data to identify location and estimated depth of unmarked burial sites. This report includes explanations of the geophysical methods, survey design, data processing and interpretation, results, and associated uncertainty. Results include figures (Appendix A) highlighting the data anomalies interpreted as burials as well as interpreted locations and depths (Appendix B).

Data collection occurred between June 30 and July 18, 2018. Logic Geophysics collected GPR data at 5 of the 6 AOCs totaling approximately 5.1 acres in total. (The City removed one AOC from the scope of work.) We used both a wheeled cart and a sled for data collection, depending on site conditions. During data collection, the GPR system tied Global Navigation Satellite System (GNSS) data directly to the incoming geophysical data for real-world positioning of the surveyed lines and detected anomalies.

Subsequent data processing produced both cross-section data profiles and depth slices. Interpretation of data anomalies provided locations (in latitude-longitude format) and depths for 403 burial sites (Appendix B). The entire project was completed safely and below budget. We appreciate the opportunity to provide these services to the City for management of this important societal and cultural resource.

2. Objectives

The objectives for this project were as follows:

- 1) Collect ground-penetrating-radar (GPR) data over 6 identified Areas of Concern (AOCs) (Figure 1):
 - a. AOC 1: Base Area (Masonic Section), 1.05 acres;
 - b. Additive Alternative (AA) #1, approximately 2.5 acres;
 - c. AA #2, approximately 1 acre;
 - d. AA #3, approximately 0.3 acres;
 - e. AA #4, approximately 0.25 acres; and
 - f. AA #5, approximately 0.4 acres.
- 2) Identify location and estimated depth of data anomalies indicative of burial sites.

Note that the City subsequently removed AA#5 from the scope of work at Logic Geophysics' suggestion due to the unsuitability of the site for achieving the survey objectives there.

3. Deliverables

Project deliverables include the following items:

- 1) Raw and processed geophysical data, if requested;
- 2) Copies of all field and daily notes, if requested;
- 3) Draft report (this document) with a description of the methods employed, containing quality maps of data anomalies interpreted as grave locations and Excel tables including both the interpreted depth and the real-world coordinates for each; and
- 4) A final report to include any amendments to the Draft Report requested by the City of Nome.

In the Work Plan, Logic Geophysics also proposed delivering geo-referenced (KMZ) maps of the collected grid, or depth slices. However, due to site conditions, the data quality was not sufficient for such maps to be useful to the city. (Note that we still provide example maps of interpreted grave anomalies in accordance with deliverable #3 above.) Instead, we are providing KMZ files containing the coordinates of interpreted burial locations. While on-site, we provided the Cemetery Manager with a tutorial on the use of these files.

4. Methods

As per the project specification, Logic Geophysics used GPR to image the subsurface at the AOCs, collecting data in a grid pattern comprised of individual parallel and perpendicular linear transects, called GPR “profiles,” within the grid. Although time intensive and therefore expensive, the grid method is the established best-practice for archaeological surveys such as this one.

4.1 Overview of the method

A GPR transmitter emits electromagnetic (EM) energy (the “signal”) into the subsurface at a specified central frequency. If conductivity is low, this signal travels as a wave. Where subsurface lithology changes, often so do electrical properties. Those changes in electrical properties can cause part of the propagating signal to reflect back to the surface. A co-located GPR receiver on the surface measures the reflected signal, which the system digitizes and records for later processing and subsequent interpretation.

GPR is often implemented for archaeological and cemetery surveys because the contrast between soil and manmade objects, such as caskets or other materials often interred with bodies,

provides amenable targets for the GPR system. Under the right conditions, bones themselves offer sufficient contrast from the background signal to identify burial locations. Experienced practitioners can also identify data patterns indicative of trenches or excavations, which can sometimes reveal grave locations where bodies may have been interred without caskets.

GPR methods are not infallible, especially for grave detection, as the targets (burials) sometimes do not have enough contrast from the background soil properties to produce a interpretable reflection event. However, GPR is widely acknowledged as the most reliable tool for burial detection and is frequently implemented throughout the world for cemetery and other archaeological surveys.

4.2 Equipment used

Logic Geophysics employed Sensors & Software's pulseEKKOPro GPR imaging system using 500-MHz antennas mounted on a wheeled cart or a sled with a GNSS receiver affixed above the midpoint of the instrument (Figure 2). The pulseEKKOPro is the industry-leading GPR imaging solution. Research and practical experience have shown that use of higher frequency antennas (from 500 MHz to 1,000 MHz) in conjunction with the grid approach is the most reliable technique for grave location.

The 500-MHz antennas provided imaging down to about 6 feet below ground surface. The data logger, or Digital Video Logger (DVL), recorded the received signals for later processing and also displayed them during data collection for real-time quality control of incoming data (Figure 3).

4.3 Survey Design

Table 1 provides GPR data parameters during collection. In accordance with the Work Plan and project specifications, grid-line spacing was 1-foot. The sample spacing along each line was 1.8 inches, offering enhanced resolution above the initial project specification.

Table 1: Data collection parameters

Parameter	Setting
Grid size	Variable
Survey type	Reflection (common offset)
Antenna polarization	Broadside
Antenna orientation	Perpendicular
Central frequency	500 MHz
Acquisition setting	Odometer
Line spacing	1 foot
Along-line measurement (trace) spacing	1.8 inches
Time window	45 ns (~6 feet)
First break offset	10%
Sampling interval	200 picoseconds
Antenna separation	0.75 feet
Stacking	DynaQ
Pulser voltage	180 Volts

A GPR setting that deserves special mention is the stacking, set to "DynaQ" (see also Figure 3). One way to improve signal-to-noise ratio for common-offset reflection GPR data is to collect more than 1 trace at each measurement position, average them, and record the average trace. This method is commonly called "stacking." Stacking improves data quality because noise tends to destructively interfere, and thus go to zero, as stacks increase. Signal, such as reflection

events, tends to constructively add together. In the Sensors & Software instrument, “DynaQ” is an advanced patented technology that adjusts the data stacking real-time depending on system speed, essentially resulting in enhanced automatic stacking of the data. System testing shows that DynaQ dramatically improves data quality over conventional stacking.

4.4 Location and Positioning

All positioning for the geophysical data used GNSS real-time kinematic (RTK) surveying techniques for optimal positioning accuracy. Due to the inaccuracy of the provided grid corner coordinates, Logic Geophysics established a GNSS base station on-site at project start-up. A GNSS antenna tied to that base station provided RTK data quality (sub-inch accuracy) for the GPR data. The GPR data logger tied incoming GNSS NMEA-data strings from the GNSS antenna directly to the GPR data for real-world positioning of collected data. The Leica GS14 roving antenna streamed GGA standard data packages to the GPR system at 1 Hz. The GNSS coordinate system is WGS84, latitude-longitude, in decimal degrees.

5. Data Quality Assurance and Quality Control (QA/QC)

5.2 QA/QC Tests

GPR data QA/QC checks included the following items:

- 1) System tests before and after data acquisition, to verify system response;
- 2) Static data collection before daily acquisition, to verify data collection parameters and qualitatively assess data quality;
- 3) Dynamic real-time monitoring of GNSS data quality during data acquisition; and
- 4) Real-time monitoring of GPR data quality via the system’s visualization of the DynaQ stacking Quality Factor (QF)

Before each line’s collection begins, the DVL displayed the system settings to ensure no unintended changes have occurred that would negatively affect data quality. The DVL simultaneously displayed the starting GNSS data quality information to ensure positioning accuracy reliability (RTK scale, Figure 3b).

Real-time GPR QA/QC is provided by visual monitoring of the incoming GPR and GNSS data in the DVL (Figure 3a). The DVL processed the incoming data for visualization purposes, but to maintain data integrity stored only the raw data. With the real-time visualization of processed data, Logic’s experienced GPR operator could readily detect problems with signal content or interference from external noise sources, such as VHF radios.

During data collection, the DVL displayed the real-time GNSS quality, ranging from RTK-Fixed to RTK to DGPS to GPS in descending order of accuracy (Figure 3b). During data collection, the system also displayed the DynaQ QF color scale, from blue to green to yellow to red (Figure 3b). Blue and green indicate higher data quality, while yellow and red indicate unacceptable data quality. Thus, the operator could immediately recollect any GPR line where the QF fell to the yellow level or below during acquisition.

5.2 QA/QC Results

All real-time QA/QC of the incoming GPR and GNSS data indicated suitable data quality. Throughout GPR acquisition, we qualitatively assessed the data quality to be fair or good, on a scale of poor-fair-good. The DynaQ QF throughout the surveys was blue, indicating the highest data quality on the DynaQ scale (Figure 3). Concerning the GNSS quality, the incoming positioning data was RTK-Fixed quality throughout 99% of data collection.

6 Project Sites

The project was located at the cemetery in Nome, Alaska (Figure 1). Logic surveyed 5 AOCs in total, comprising about 5.1 acres surveyed (Table 2). AOC size and site conditions, including obstructions, dictated individual grid sizes within each AOC. Maximum grid size employed was 115 feet by 100 feet, due to data processing and visualization considerations.

6.1 Base Area (Masonic Section)

The Base Area was approximately 1.05 acres in size. The corners of this AOC, as confirmed with the cemetery manager, were marked by 4 tall posts. Many known burials were present at this site, as indicated by grave markers and grave enclosures. The surface was mostly level, with grasses of varying heights throughout. We used the cart for data collection throughout the Base Area.

The Base Area surveys comprised 7 grids total, ranging in size from approximately 3,000 square feet to 8,000 square feet. Grave markers, grave enclosures, a small building, and a gravel pile on the AOC all obstructed surveys to varying extents.

6.2 AA1

AA1 was approximately 2.5 acres in size. The cemetery manager delineated the outline of this AOC using existing lathe markers on the northern and western sides and placing flagging on the southwestern and western boundaries. Two roads formed the southernmost boundary.

7 grave markers within this AOC indicated the location of known burials. The site surface was highly variable. In the northeastern corner of the AOC, the surface was tundra with tussocks present as high as 2 feet above mean elevation level. In the southwestern portion of the site, the surface was grassy. Willow trees initially covered much of the area in the central and western sections of this AOC. The City removed the willows and then bulldozed the site to enable GPR data collection. We used the sled for data collection throughout AA1.

The AA1 surveys comprised 14 grids total, ranging in size from about 2,000 square feet to 11,500 square feet. Some obstructions still precluded total coverage, including the existing grave markers and large holes apparently of human origin.

6.3 AA2

AA2 was approximately 1 acre in size. Roads delineated the AOC boundary to the north, east, and west. The cemetery manager flagged the southern boundary, and grass mowing was accomplished with the flagged area. The site surface was variable. In the eastern section of the AOC, the surface was mostly dirt and was very uneven, having holes, rises, and dips throughout. We used the sled for data collection throughout this portion of AA2. In the western half of AA2, the surface was not level but was grassy and firm, so we were able to use the cart for surveying.

The AA2 surveys comprised 6 grids total, ranging in size from about 4,500 square feet to 6,300 square feet in size. Many grave markers and existing graves as well as surface roughness obstructed the surveys to varying degrees at this site.

6.4 AA3

AA3 was approximately 0.3 acres in size. Roads delineated the southern, eastern, and western boundaries of this site. The cemetery manager placed flagging to delineate the northern survey boundary of AA3. The AA3 surveys comprised 3 grids. The site surface was mostly level and grassy. However, many grave markers in place within this AOC obstructed the GPR surveys. We used the cart for data collection at AA3.

6.5 AA4

AA4 was approximately 0.25 acres in size. A road delineated its eastern boundary, while the cemetery manager delineated the western boundary. No grave markers existed within this AOC. The site surface was mostly level and grassy. We used the cart for data collection at this site. The AA4 surveys comprised 1 grid.

Table 2: AOC survey information

AOC	Approximate Area Surveyed	Number of Grids Completed	Approximate Line Miles Surveyed	Days to Complete
Base Area	1.05	7	14	3
AA1	2.5	14	36	10
AA2	1	6	13	3
AA3	0.3	3	5	1
AA4	0.25	1	4	1
Totals	5.1	31	72	18

7. Data Analysis

7.1 Initial Processing

After data collection, we downloaded the data from the DVL onto the processing computer. We used Sensors & Software EKKOProjects software for data processing and visualization. The steps below provide a summary of the data processing workflow:

- 1) Delete bad traces: We deleted traces with zero information content, excessive noise, or bad GNSS data. Besides deleting bad traces, we did not apply any corrections for positioning offsets, due to the high quality of the GNSS data as discussed previously.
- 2) Dewow: Dewow is a zero-phase filter generating the difference between the trace value and the average trace value over a defined window width. Dewow removes unwanted “wow” from the GPR trace while preserving high-frequency signal. Wow is a slowly decaying, low-frequency signal that may be induced on the trace due to the proximity of transmitter and receiver and the electrical properties of the ground. GPR data require the dewow process before viewing or carrying out further processing.
- 3) Repicking the “first break”: Repicking the first break is a static shift to determine the time where the signal crosses the defined threshold for each trace, that is, the true “zero time.” The algorithm shifted all traces equally in time to align the median value of the first break times with zero time. The algorithm threshold was 5 mV.
- 4) Background subtraction: This process is a 2-dimensional spatial filter. The filter calculated the average trace and subtracted the average trace from every data trace. This filter removed the direct arrival between the 2 antennas, the uppermost band of data, that can blank out very near-surface reflectors. It also removed other static noise in the data, likely caused by the proximity of the GNSS antenna.
- 5) Velocity analysis: Determining the correct radar wave velocity is essential for accurate determination of object depth and for migration processing (Step 6, below). We used a hyperbolic velocity calibration to fit a superimposed hyperbola to diffraction patterns in the data, where present. The software then estimated the radar wave velocity from the parameters of the hyperbola.

- 6) F-K migration: The F-K migration applied a synthetic aperture image reconstruction process to each GPR line. The algorithm computes the Fourier transform of the GPR data into plane waves at a monochromatic frequency. This process superimposes reflection energy to the correct source point and moves dipping reflectors to their true subsurface position. For optimal results, migration requires the input velocity to be as accurate as possible. We used the velocity calculated in Step 5.
- 7) Gain: Since radar signal strength decreases with time due to unavoidable attenuation processes, applying a gain function boosted the later time signals for optimal visualization and interpretation. We used spreading and exponential compensation (SEC) gain, a composite of linear time gain and exponential signal recovery, to optimize late-time reflection events. This gain attempts to compensate both for spherical spreading losses and for the exponential ohmic dissipation of EM energy. SEC gain is the gain closest to physical reality and most commonly used for GPR data.

We derived depth estimates of targets using the “first-break,” that is, the first deviation from zero position of the target reflection wavelet. Although many practitioners use the middle of the wavelet rather than the first break, research has shown that the first break provides the correct depth estimate while the middle pick does not.

7.2 Plotting and Interpretation

Typically, practitioners display GPR data in profiles, where the x-axis is position (in odometer mode) or trace number (in free-run mode) along the profile and the y-axis is depth or time. The plots are typically greyscale, but research has shown that color profile plots are more conducive to interpretation. Therefore, we use a typical seismic color plot rather than greyscale, with the amplitude colors ranging from blue (negative) to white (zero) to red (positive). In processed profiles, the colors represent normalized amplitudes, which are unitless. The profile figures in this report do not include color bars, as is standard for GPR profile plots (Figure 4).

After processing, EKKOProjects gridded the individual profile data together to visualize in depth slices from a map view, rather than just a profile view. Processing the data as a series of depth slices usually enhances interpretation of GPR data, providing visualization of coherent anomalies associated with the targets of interest, that is, unmarked burials. The depth slices provide an image of the average normalized (no negative values) GPR amplitude values in the specified thickness, or depth range.

However, due in large part to the surface roughness throughout the sites, in most cases the data maps were not useful for data interpretation. Therefore, we went through each data set line by line, looking for data anomalies indicative of burials. Then, we used the GNSS data to extrapolate coordinates for those anomalies. Finally, we compiled spreadsheets of interpreted anomaly locations, in latitude-longitude format, and anomaly depths. (We ignored any anomalies within the first 2 feet of the surface, as those anomalies were likely correlated with the thawed/frozen interface rather than burials.) Converting these spreadsheets into KMZ files provided a deliverable that the City can view in Google Earth or other georeferenced databases, for future cemetery management.

8. Results

8.1 Interpreted burial locations and depths

Appendix B contains tables of interpreted grave locations for each AOC. The corresponding KMZ files are being delivered with this report. In total, we identified 403 anomalies in the GPR data

that may indicate burial locations (Table 3). In some cases, especially at the Base Area, some anomaly locations may be correlated with existing marked graves. It is important to note when examining the maps that the Google Earth projection is shifted from real-world locations.

Table 3: Summary showing number of anomalies located in each AOC

AOC	Total Anomalies
Base Area	145
AA1	116
AA2	107
AA3	20
AA4	15
Total	403

8.1 Base Area (Masonic Section)

The base area contained 145 interpreted anomalies. Notably, the northeastern-most 4,000 square feet of this area has minimal interpreted burial locations and appears to be mostly undisturbed ground (Figure 5).

8.2 AA1

We interpreted 116 anomalies in AA1 to be indicative of potential burial sites (Figure 6). These anomalies ranged from 2 feet to 6 feet below surface. Some of these anomalies may be indicative of other anthropogenic activities, such as old mining holes and even previous runway lighting systems, but we erred on the side of caution when interpreting anomalies in this area.

8.3 AA2

Even though it was 60% smaller than AA1, AA2 contained 107 anomalies likely indicative of burial locations, a much higher potential burial density (Figure 7). This result is corroborated by the fact that AA2 is obviously used for current and historic burials, whereas AA1 for the most part has little surface expression of potential burials.

8.4 AA3

AA3 contained 29 anomalies interpreted to be indicative of potential burials (Figure 8). Some anomalies within AA3 were found to exist very close to existing grave markers, yet appearing to be associated with a separate burial.

8.5 AA4

In AA4, we interpreted 15 anomalies likely to be indicative of burial locations, some within just a few feet of the existing roadway (Figure 9).

8.2 Sources of Error and Uncertainty Analysis

Several potential sources of error exist for these data and this analysis. Here we list 3 relevant sources of errors and corresponding considerations.

- 1) Depth errors: For the GPR method, converting the data, measured in time, into depth, is likely the largest source of error. The time-to-depth conversions will be only as accurate as the velocity estimate. Furthermore, incorrect velocity can limit the efficacy of the migration and gridding algorithms essential for viewing the data.

Reliably estimating the radar-wave velocity, and therefore anomaly depths, is complicated by the surface roughness present throughout the site. Additionally, in the Arctic, the subsurface velocity structure can be highly variable laterally and vertically. For example, the velocity of the thawed layer can be half the velocity of the underlying permafrost. As a consequence, where the thickness of the thawed layer changes, so does the overall velocity profile of the subsurface. Compensating for this factor is outside the scope of this work. As a result, we estimate the potential error in the overall velocity estimates to be $\pm 20\%$, with the corresponding error in the depth estimates. Due to this large uncertainty, we only report depth estimates in integer values.

- 2) Position errors: Errors in estimates of anomaly position are often linked. These errors can originate from several sources including the following:
 - 1) Horizontal resolution limitations;
 - 2) Spatial sampling density; and
 - 3) Positioning errors of the geophysical data within the grid.

We attempted to minimize travel path errors by traveling between marked points during GPR surveys. During survey set-up, we marked the outer grid lines with a measuring tape and paint. Then, during acquisition, the operator placed a lathe on the end of the line to be traveled, and aimed directly at that lathe while traveling down the line. To mitigate problems associated with spatial resolution, we set the sampling density to about twice that required for 500-MHz data (Table 1). Concerning positioning errors, the RTK-quality GNSS data was accurate to within inches. However, surface roughness at some of the sites (AA1 and AA2) induced movement of the GNSS antenna on the order of a foot or more, with corresponding uncertainty in data positioning.

Horizontal resolution limitations are an unavoidable consequence of the physics behind GPR. We can calculate the horizontal resolution to estimate uncertainty in anomaly positions via known equations. Calculations using these site conditions and 500-MHz antennas reveals that the horizontal resolution at 5 to 6 feet depth is on the order of 6 inches.

- 3) Site Conditions: At the Nome cemetery, several on-site considerations can give rise to both false positive responses (burials indicated where burials are not present) or false negative responses (no burial indicated where a burial is present). For example, where manmade holes were filled in before the surveys in AA1 and AA2, the GPR data over those locations may appear similar to GPR data responses from graves.

Obviously, the latter response (false negative) is more concerning for cemetery management. False negatives can arise from multiple sources:

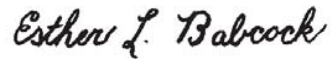
- 1) Surface roughness can prevent burial anomalies from appearing coherent and therefore distinguishable from background reflection events in the GPR data.
- 2) Where bodies are interred without caskets, the reflection strength of the GPR signal from the body itself may not be strong enough to distinguish from the background signal, since the electrical properties of bone are not extremely different from soil, especially as compared to, for example, metallic objects in soil.
- 3) Where multiple soil layers are present, such as is the case in the permafrost environment in Nome, reflections from within the soil itself may interrupt reflections from bodies and therefore preclude detection.

In spite of these considerations, as mentioned earlier, GPR is widely regarded as the most reliable method for detecting human burials. Our careful data processing and our expertise in GPR data interpretation also helps to reduce the chances for false responses.

9. Conclusions

Logic Geophysics conducted GPR surveys at the City's cemetery in Nome, Alaska, successfully identifying 403 anomalies likely associated with burials. Logic Geophysics & Analytics LLC is pleased to provide this report to the City of Nome to aid the management of this important cultural and societal resource. Please contact me if you have any questions.

Sincerely,



Esther Babcock, Ph.D.

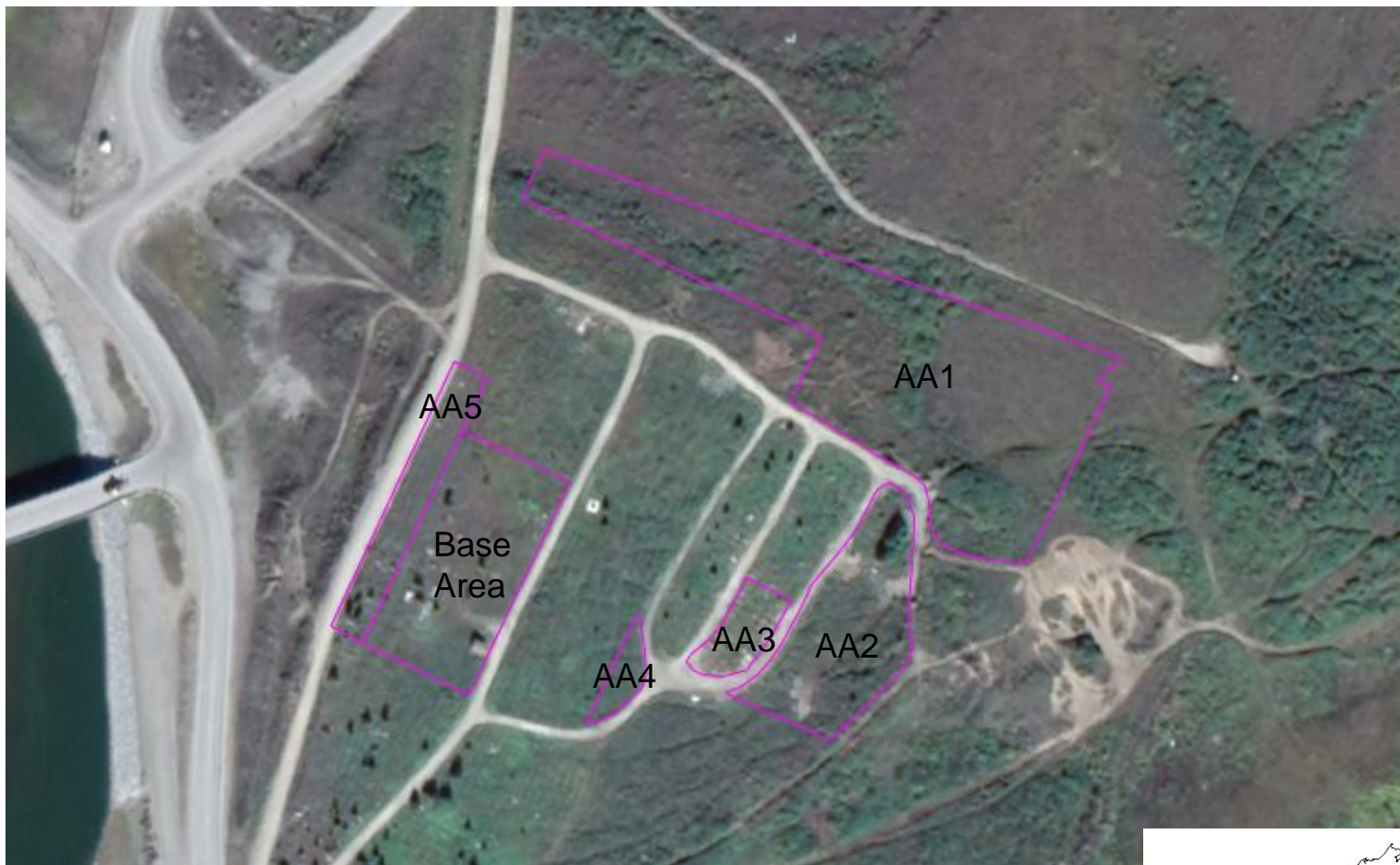
President/Chief Geophysicist

Logic Geophysics & Analytics LLC

ebabcock@logicgeophysics.com | Ph: (907) 744-8111

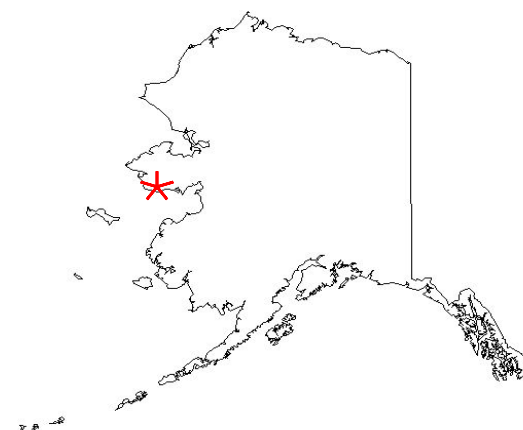
Service Disabled Veteran Owned – Certified Alaska DOT DBE – Woman Owned Small Business

Appendix A



500 Feet

— Area Outlines

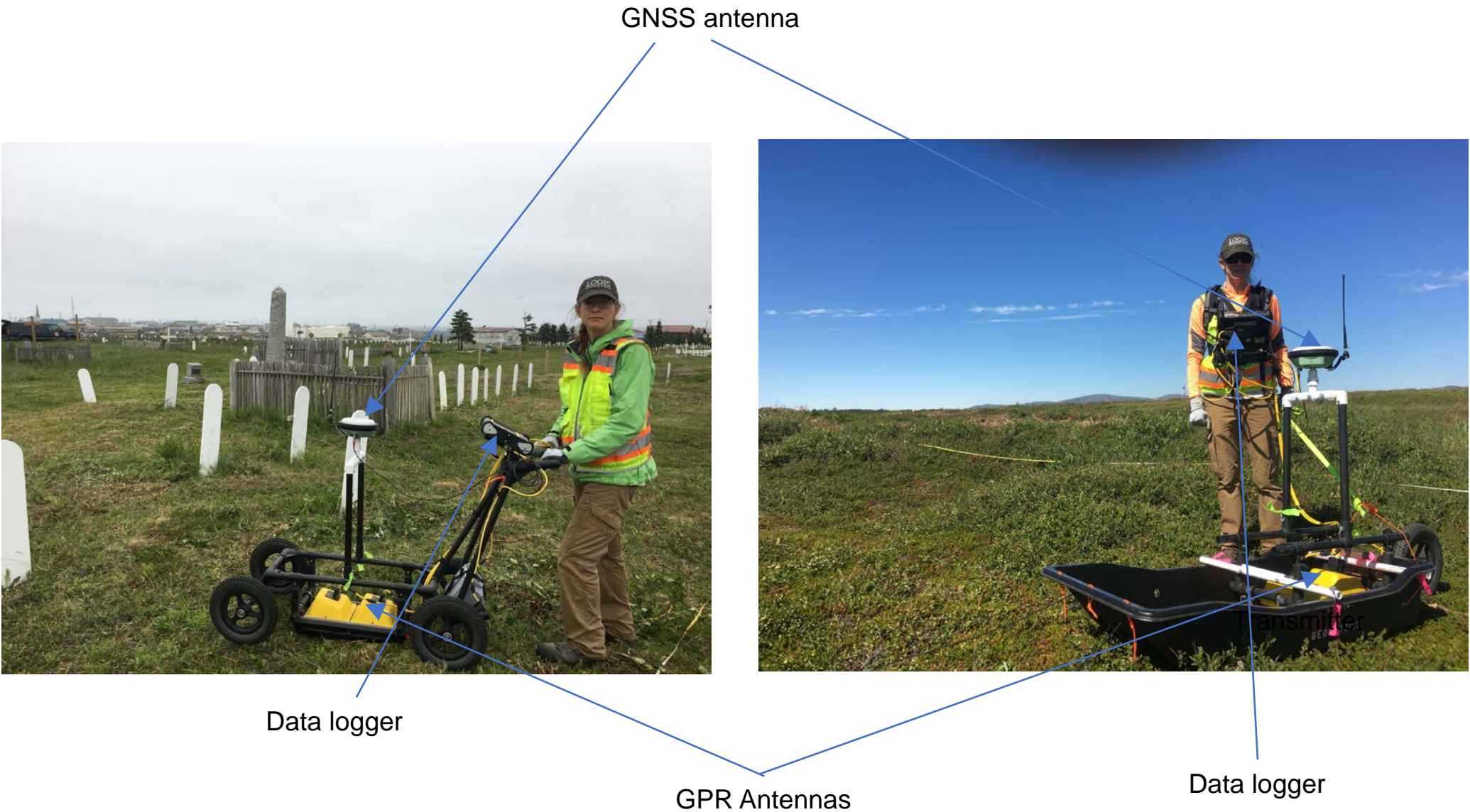


Ground-Penetrating-Radar Surveys at the City Cemetery

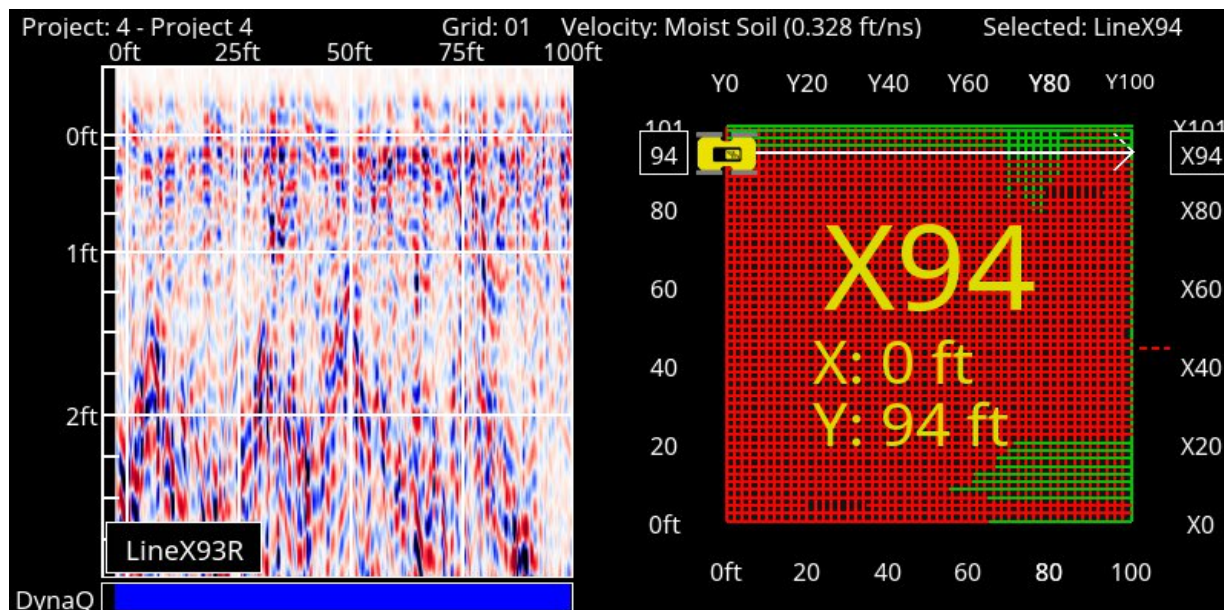
Location: Nome, Alaska

Client: City of Nome

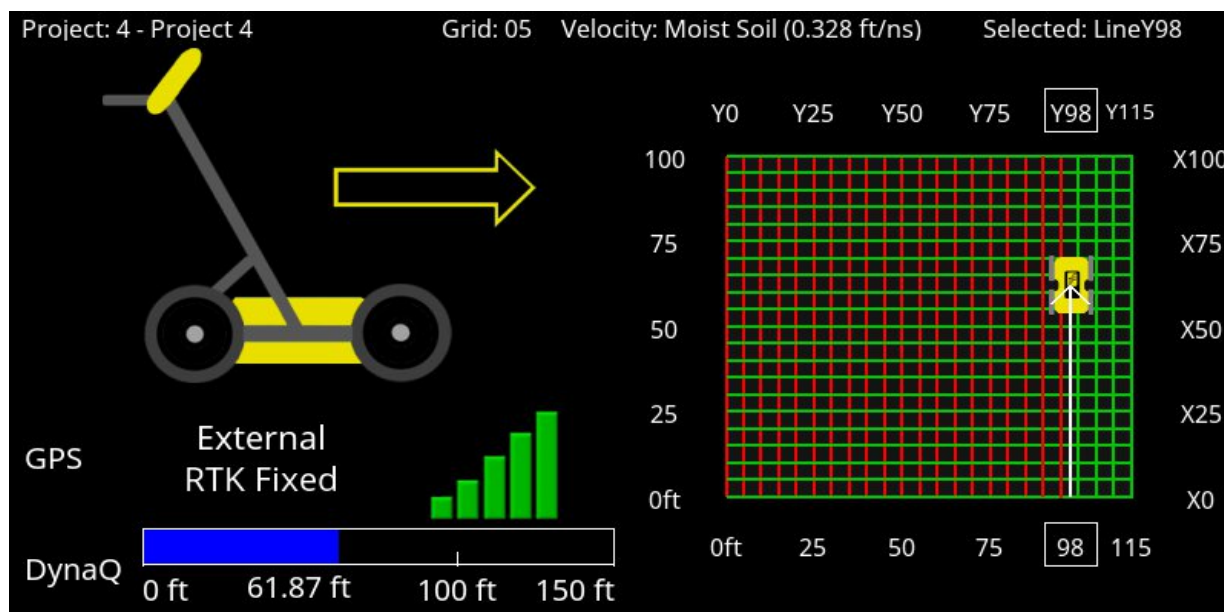
Site Overview from Google Earth Imagery



Ground-Penetrating-Radar Surveys at the City Cemetery	
Location: Nome, Alaska	Client: City of Nome
GPR Equipment On-Site	



a) The data logger display starting data collection; the left half shows the previous collected data in profile view, enable real-time quality control during acquisition; note the DynaQ color scale below the profile as described in the text. The right half shows the grid, collected lines, and current line position.



b) The data logger display during data collection; note the GPS and DynaQ data quality indicators on the bottom of the left panel. The GNSS data quality is indicated both by the notation ("RTK Fixed") and the green bars (number of received satellites).

*Red lines are collected data; green lines have yet to be collected.

Ground-Penetrating-Radar Surveys at the City Cemetery

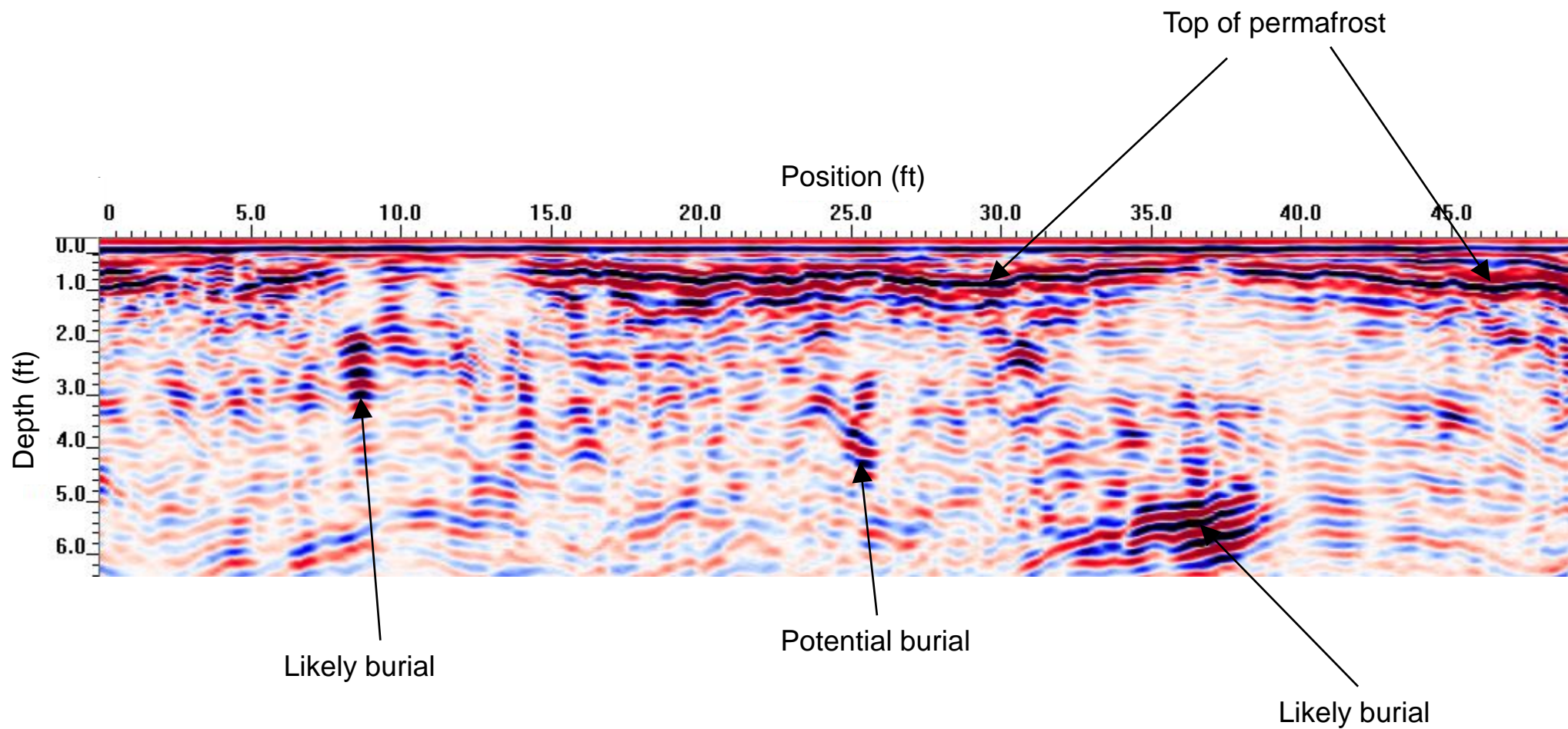
Location: Nome, Alaska

Client: City of Nome

Example of Data Logger Displays and QA/QC During Collection

Fig.

3



Ground-Penetrating-Radar Surveys at the City Cemetery

Location: Nome, Alaska

Client: City of Nome

Example Profile Data

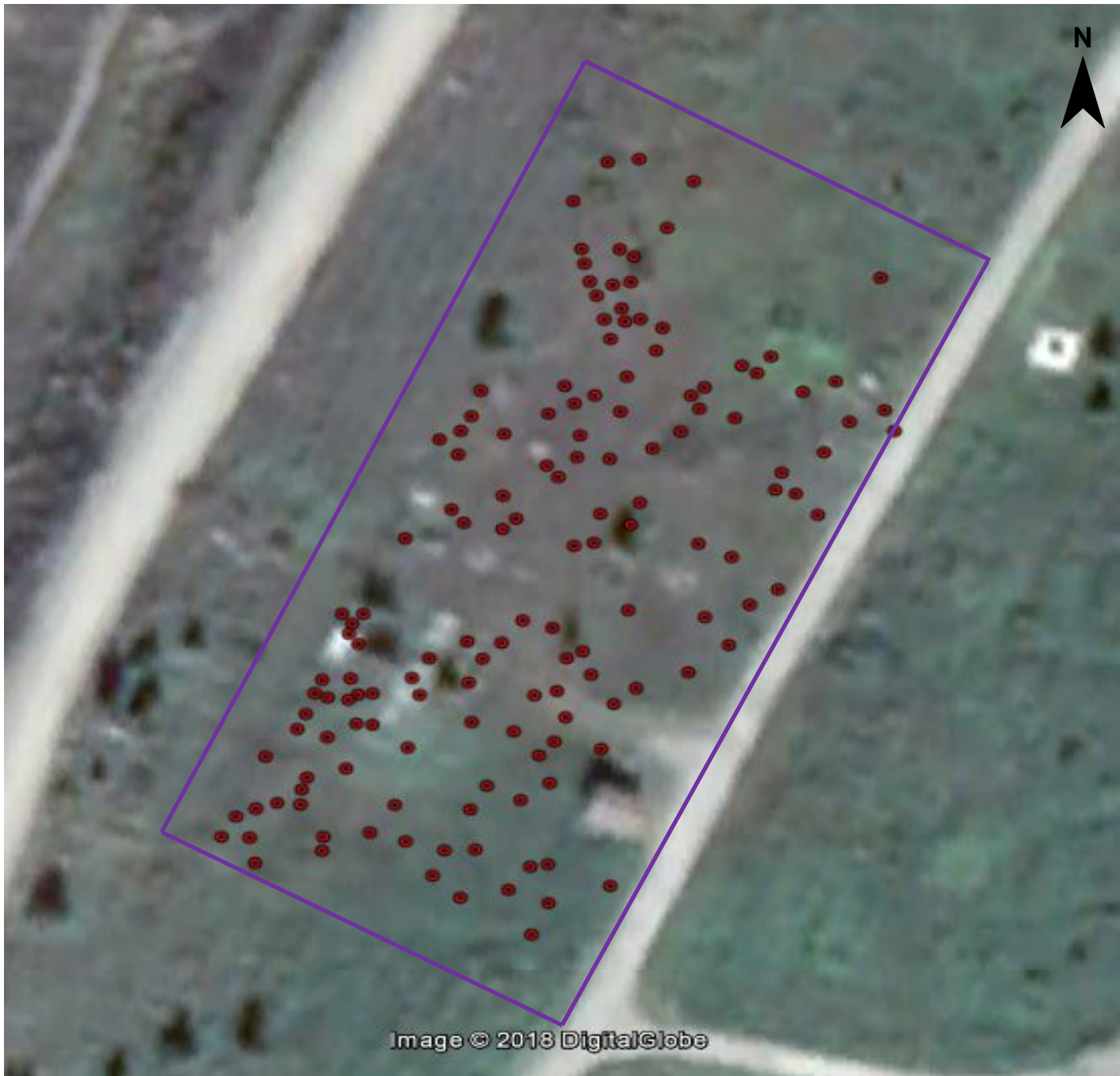
Fig.

4

100 Feet

● Interpreted Potential Burial Location

— Approximate Base Area Survey Boundary



Ground-Penetrating-Radar Surveys at the City Cemetery	
Location: Nome, Alaska	Client: City of Nome
Interpreted Anomaly Map: Base Area	



Ground-Penetrating-Radar Surveys at the City Cemetery

Location: Nome, Alaska

Client: City of Nome

Interpreted Anomaly Map: AA1

100 Feet

● Interpreted Potential Burial Location

— Approximate AA2 Survey Boundary



Ground-Penetrating-Radar Surveys at the City Cemetery

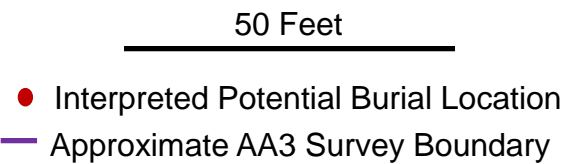
Location: Nome, Alaska

Client: City of Nome

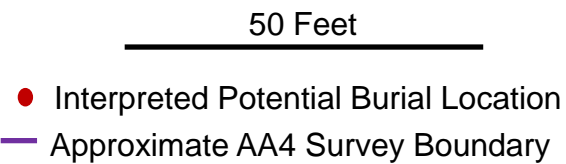
Interpreted Anomaly Map: AA2

Fig.

7



Ground-Penetrating-Radar Surveys at the City Cemetery	
Location: Nome, Alaska	Client: City of Nome
Interpreted Anomaly Map: AA3	



Ground-Penetrating-Radar Surveys at the City Cemetery	
Location: Nome, Alaska	Client: City of Nome
Interpreted Anomaly Map: AA4	

Appendix B

Base Area Anomaly Locations and Depths

Latitude	Longitude	Name	Depth
64.5049995 N	165.4209336 W	BA-G1-1	3
64.5049241 N	165.4205609 W	BA-G1_4	4
64.5049901 N	165.4208591 W	BA-G1_5	4
64.5049813 N	165.4207138 W	BA-G1_6	4
64.5049805 N	165.4207783 W	BA-G1_7	4
64.5049630 N	165.4205994 W	BA-G1_9	4
64.5048904 N	165.4205967 W	BA-G1_10	4
64.5049382 N	165.4206447 W	BA-G1_11	5
64.5049424 N	165.4204325 W	BA-G1_14	5
64.5049299 N	165.4207451 W	BA-G1_15	5
64.5049535 N	165.4208028 W	BA-G1_17	5
64.5050290 N	165.4208817 W	BA-G1_18	5
64.5049656 N	165.4205624 W	BA-G1_19	5
64.5051597 N	165.4207275 W	BA-G2_1	3
64.5050887 N	165.4204510 W	BA-G2_2	3
64.5050524 N	165.4205586 W	BA-G2_3	3
64.5050967 N	165.4205490 W	BA-G2_4	3
64.5051369 N	165.4204250 W	BA-G2_6	3
64.5051462 N	165.4205907 W	BA-G2_7	4
64.5051507 N	165.4205435 W	BA-G2_9	4
64.5050903 N	165.4208545 W	BA-G2_10	3
64.5051857 N	165.4208100 W	BA-G2_11	3
64.5051852 N	165.4206986 W	BA-G2_12	3
64.5050495 N	165.4206897 W	BA-G2_13	4
64.5050342 N	165.4206192 W	BA-G2_14	4
64.5051682 N	165.4204724 W	BA-G2_15	3
64.5051227 N	165.4205256 W	BA-G2_17	3
64.5051931 N	165.4204900 W	BA-G2_18	3
64.5050819 N	165.4205811 W	BA-G2_20	4
64.5051860 N	165.4205233 W	BA-G2_21	4
64.5051175 N	165.4207213 W	BA-G2_22	3
64.5052023 N	165.4206590 W	BA-G2_23	4
64.5051465 N	165.4208297 W	BA-G2_24	4
64.5051647 N	165.4208459 W	BA-G2_25	5
64.5051413 N	165.4209785 W	BA-G2_28	5
64.5052010 N	165.4209572 W	BA-G2_30	4
64.5051482 N	165.4209277 W	BA-G2_31	4
64.5051076 N	165.4206337 W	BA-G2_32	4
64.5052035 N	165.4207307 W	BA-G2_36	4
64.5051538 N	165.4203785 W	BA-G3_1	3
64.5052297 N	165.4202351 W	BA-G3_3	3
64.5053082 N	165.4202487 W	BA-G3_4	3
64.5052939 N	165.4201796 W	BA-G3_5	3
64.5053658 N	165.4200884 W	BA-G3_8	4
64.5052183 N	165.4205528 W	BA-G3_9	4
64.5052372 N	165.4203950 W	BA-G3_10	4
64.5051707 N	165.4202698 W	BA-G3_11	4
64.5054100 N	165.4203443 W	BA-G3_12	4
64.5053092 N	165.4204665 W	BA-G3_13	4

64.5053390 N	165.4199997 W	BA-G3_14	4
64.5053616 N	165.4200458 W	BA-G3_15	4
64.5052593 N	165.4200826 W	BA-G3_16	5
64.5052429 N	165.4201416 W	BA-G3_17	5
64.5053285 N	165.4203902 W	BA-G3_18	5
64.5051998 N	165.4201854 W	BA-G3_19	5
64.5054665 N	165.4202641 W	BA-G4_2	3
64.5054060 N	165.4199865 W	BA-G4_3	4
64.5054705 N	165.4200312 W	BA-G4_5	4
64.5054905 N	165.4201269 W	BA-G4_6	4
64.5054524 N	165.4202467 W	BA-G4_7	4
64.5054281 N	165.4202854 W	BA-G4_8	4
64.5054425 N	165.4201731 W	BA-G4_9	4
64.5053842 N	165.4200752 W	BA-G4_10	4
64.5054286 N	165.4198399 W	BA-G4_11	4
64.5055081 N	165.4200975 W	BA-G4_13	4
64.5054753 N	165.4202361 W	BA-G4_15	5
64.5054385 N	165.4199338 W	BA-G4_16	5
64.5055923 N	165.4198690 W	BA-G4_17	5
64.5054508 N	165.4198606 W	BA-G4_18	5
64.5054815 N	165.4199626 W	BA-G4_19	5
64.5054985 N	165.4201583 W	BA-G4_20	5
64.5050295 N	165.4210781 W	BA-G5_2	3
64.5049950 N	165.4212425 W	BA-G5_4	3
64.5049801 N	165.4210330 W	BA-G5_7	3
64.5050680 N	165.4209831 W	BA-G5_9	3
64.5051642 N	165.4209735 W	BA-G5_10	4
64.5051484 N	165.4210480 W	BA-G5_11	4
64.5051263 N	165.4210671 W	BA-G5_12	4
64.5049940 N	165.4211842 W	BA-G5_13	4
64.5052334 N	165.4209912 W	BA-G5_16	4
64.5050312 N	165.4211266 W	BA-G5_17	4
64.5049950 N	165.4210304 W	BA-G5_18	4
64.5051469 N	165.4209580 W	BA-G5_19	5
64.5050582 N	165.4210647 W	BA-G5_20	5
64.5050456 N	165.4210756 W	BA-G5_21	5
64.5050251 N	165.4211709 W	BA-G5_22	5
64.5050166 N	165.4212123 W	BA-G5_23	5
64.5052119 N	165.4209770 W	BA-G5_24	5
64.5052227 N	165.4209702 W	BA-G5_25	5
64.5050807 N	165.4211509 W	BA-G5_26	5
64.5051101 N	165.4210849 W	BA-G5_29	5
64.5049671 N	165.4211727 W	BA-G5_33	5
64.5051013 N	165.4210224 W	BA-G5_35	6
64.5051147 N	165.4209284 W	BA-G5_36	6
64.5051158 N	165.4209616 W	BA-G5_37	6
64.5051628 N	165.4210330 W	BA-G5_39	6
64.5051437 N	165.4210216 W	BA-G5_40	6
64.5054035 N	165.4207494 W	BA-G6_1	2
64.5052262 N	165.4206148 W	BA-G6_3	2

64.5054472 N	165.4205615 W	BA-G6_5	2
64.5052332 N	165.4209471 W	BA-G6_7	3
64.5053138 N	165.4208594 W	BA-G6_8	3
64.5053594 N	165.4206560 W	BA-G6_10	4
64.5053305 N	165.4207378 W	BA-G6_11	4
64.5053059 N	165.4205080 W	BA-G6_12	4
64.5053795 N	165.4205408 W	BA-G6_13	4
64.5054718 N	165.4207020 W	BA-G6_14	4
64.5054239 N	165.4204955 W	BA-G6_15	4
64.5054287 N	165.4207440 W	BA-G6_16	4
64.5054444 N	165.4207221 W	BA-G6_17	4
64.5053989 N	165.4204335 W	BA-G6_20	4
64.5053520 N	165.4203710 W	BA-G6_21	4
64.5053917 N	165.4205647 W	BA-G6_22	5
64.5054007 N	165.4205015 W	BA-G6_23	5
64.5053402 N	165.4204531 W	BA-G6_24	5
64.5054197 N	165.4207882 W	BA-G6_25	5
64.5053447 N	165.4207633 W	BA-G6_26	5
64.5054580 N	165.4205071 W	BA-G6_30	6
64.5054255 N	165.4206538 W	BA-G6_31	6
64.5053349 N	165.4206287 W	BA-G6_32	6
64.5053239 N	165.4206570 W	BA-G6_33	6
64.5055387 N	165.4203233 W	BA-G7_1	2
64.5056228 N	165.4204126 W	BA-G7_2	2
64.5054494 N	165.4204113 W	BA-G7_3	3
64.5057192 N	165.4203722 W	BA-G7_4	3
64.5054667 N	165.4204647 W	BA-G7_5	3
64.5056232 N	165.4204923 W	BA-G7_9	3
64.5054867 N	165.4203980 W	BA-G7_10	3
64.5054767 N	165.4205277 W	BA-G7_11	3
64.5055201 N	165.4203230 W	BA-G7_12	3
64.5055270 N	165.4204321 W	BA-G7_15	4
64.5056955 N	165.4202586 W	BA-G7_17	4
64.5056743 N	165.4205098 W	BA-G7_19	4
64.5057160 N	165.4204378 W	BA-G7_20	4
64.5056459 N	165.4203138 W	BA-G7_24	5
64.5055146 N	165.4203369 W	BA-G7_25	5
64.5055480 N	165.4204450 W	BA-G7_26	5
64.5055848 N	165.4204274 W	BA-G7_28	5
64.5055457 N	165.4204017 W	BA-G7_29	5
64.5055733 N	165.4204608 W	BA-G7_31	5
64.5055883 N	165.4204750 W	BA-G7_32	5
64.5056150 N	165.4203832 W	BA-G7_33	6
64.5055596 N	165.4204089 W	BA-G7_34	6
64.5056075 N	165.4204864 W	BA-G7_35	6
64.5055879 N	165.4203897 W	BA-G7_36	6

AA1 Anomaly Locations and Depths

Latitude	Longitude	Name	Depth
64.5060093 N	165.4157688 W	AA1-G1_1	3
64.5057935 N	165.4156105 W	AA1-G1_3	3
64.5060452 N	165.4157102 W	AA1-G1_4	3
64.5058257 N	165.4160104 W	AA1-G1_8	5
64.5057389 N	165.4154848 W	AA1-G1_10	6
64.5058932 N	165.4153036 W	AA1-G1_11	5
64.5057666 N	165.4155603 W	AA1-G1_13	4
64.5058869 N	165.4154637 W	AA1-G1_14	6
64.5058197 N	165.4158654 W	AA1-G1_16	4
64.5058440 N	165.4154151 W	AA1-G1_18	6
64.5058892 N	165.4158799 W	AA1-G1_19	5
64.5056774 N	165.4159140 W	AA1-G2_1	3
64.5056774 N	165.4157070 W	AA1-G2_2	3
64.5056452 N	165.4160377 W	AA1-G2_3	3
64.5056693 N	165.4160899 W	AA1-G2_4	3
64.5057539 N	165.4159240 W	AA1-G2_6	4
64.5057154 N	165.4155449 W	AA1-G2_8	5
64.5054881 N	165.4157145 W	AA1-G2_9	6
64.5057229 N	165.4160324 W	AA1-G2_11	6
64.5056454 N	165.4156843 W	AA1-G2_12	5
64.5055732 N	165.4158644 W	AA1-G2_14	6
64.5055663 N	165.4157902 W	AA1-G2_15	5
64.5056199 N	165.4159254 W	AA1-G2_16	6
64.5053373 N	165.4159855 W	AA1-G3_1	3
64.5054573 N	165.4158109 W	AA1-G3_2	4
64.5054455 N	165.4157300 W	AA1-G3_4	5
64.5054325 N	165.4158712 W	AA1-G3_5	5
64.5053685 N	165.4158919 W	AA1-G3_7	5
64.5053464 N	165.4158357 W	AA1-G3_8	6
64.5059703 N	165.4165272 W	AA1-G5_2	5
64.5060492 N	165.4160603 W	AA1-G5_3	6
64.5061334 N	165.4163930 W	AA1-G5_5	5
64.5060904 N	165.4161959 W	AA1-G5_6	5
64.5060699 N	165.4164772 W	AA1-G5_7	5
64.5059931 N	165.4161534 W	AA1-G5_8	5
64.5059634 N	165.4160441 W	AA1-G5_9	5
64.5060414 N	165.4165761 W	AA1-G5_12	4
64.5057061 N	165.4165832 W	AA1-G6_1	5
64.5057050 N	165.4162220 W	AA1-G6_3	4
64.5057017 N	165.4163060 W	AA1-G6_5	4
64.5057923 N	165.4162543 W	AA1-G6_6	4
64.5057497 N	165.4164398 W	AA1-G6_7	4
64.5058545 N	165.4166109 W	AA1-G6_9	3
64.5057974 N	165.4174158 W	AA1-G7_2	4
64.5058730 N	165.4177077 W	AA1-G7_3	3
64.5059103 N	165.4176051 W	AA1-G7_5	4
64.5058620 N	165.4173980 W	AA1-G7_6	3
64.5058747 N	165.4172586 W	AA1-G7_9	5
64.5059800 N	165.4175590 W	AA1-G7_11	4

64.5059167 N	165.4172541 W	AA1-G7_13	2
64.5059732 N	165.4172284 W	AA1-G7_15	2
64.5060560 N	165.4173931 W	AA1-G7_16	3
64.5060632 N	165.4175723 W	AA1-G7_18	3
64.5059176 N	165.4177306 W	AA1-G7_19	4
64.5060079 N	165.4176052 W	AA1-G7_20	4
64.5060127 N	165.4174786 W	AA1-G7_22	3
64.5059741 N	165.4174936 W	AA1-G7_24	4
64.5059339 N	165.4175176 W	AA1-G7_26	4
64.5058742 N	165.4175377 W	AA1-G7_28	5
64.5059255 N	165.4173585 W	AA1-G7_29	3
64.5059737 N	165.4171482 W	AA1-G7_31	3
64.5059093 N	165.4171231 W	AA1-G7_33	3
64.5065919 N	165.4197365 W	AA1-G8_1	3
64.5066293 N	165.4194736 W	AA1-G8_2	3
64.5065987 N	165.4193149 W	AA1-G8_5	4
64.5064867 N	165.4192400 W	AA1-G8_6	4
64.5065761 N	165.4193686 W	AA1-G8_7	4
64.5065533 N	165.4191950 W	AA1-G8_8	5
64.5064988 N	165.4193895 W	AA1-G8_9	4
64.5065270 N	165.4194850 W	AA1-G8_11	4
64.5064956 N	165.4193089 W	AA1-G8_12	4
64.5066161 N	165.4194031 W	AA1-G8_14	4
64.5066094 N	165.4196836 W	AA1-G8_16	3
64.5065744 N	165.4197107 W	AA1-G8_17	3
64.5065683 N	165.4196349 W	AA1-G8_18	5
64.5066011 N	165.4196101 W	AA1-G8_19	4
64.5065527 N	165.4195425 W	AA1-G8_20	4
64.5065383 N	165.4193071 W	AA1-G8_23	5
64.5065455 N	165.4189847 W	AA1-G9_1	3
64.5065126 N	165.4189158 W	AA1-G9_3	3
64.5065162 N	165.4187475 W	AA1-G9_5	3
64.5064482 N	165.4185749 W	AA1-G9_6	3
64.5064776 N	165.4187847 W	AA1-G9_7	3
64.5064867 N	165.4185976 W	AA1-G9_9	4
64.5064249 N	165.4187945 W	AA1-G9_10	4
64.5065019 N	165.4186883 W	AA1-G9_11	4
64.5064454 N	165.4190605 W	AA1-G9_12	5
64.5064010 N	165.4181063 W	AA1-G10_1	2
64.5064853 N	165.4184892 W	AA1-G10_2	4
64.5062630 N	165.4180921 W	AA1-G10_3	4
64.5063256 N	165.4183723 W	AA1-G10_4	4
64.5064108 N	165.4184009 W	AA1-G10_5	5
64.5060969 N	165.4166806 W	AA1-G11_1	4
64.5062489 N	165.4172042 W	AA1-G11_2	4
64.5061586 N	165.4169042 W	AA1-G11_3	4
64.5060497 N	165.4167096 W	AA1-G11_4	4
64.5061581 N	165.4165406 W	AA1-G11_5	5
64.5061853 N	165.4173051 W	AA1-G11_6	3
64.5059497 N	165.4168304 W	AA1-G12_1	4

64.5058692 N	165.4169636 W	AA1-G12_2	4
64.5059016 N	165.4168161 W	AA1-G12_3	4
64.5059927 N	165.4168130 W	AA1-G12_4	5
64.5057187 N	165.4171519 W	AA1-G12_5	2
64.5059498 N	165.4169868 W	AA1-G12_6	2
64.5058403 N	165.4171543 W	AA1-G12_7	3
64.5057679 N	165.4169315 W	AA1-G12_8	5
64.5055147 N	165.4160391 W	AA1-G13_1	3
64.5054702 N	165.4159865 W	AA1-G13_2	4
64.5062495 N	165.4178204 W	AA1-G14_1	3
64.5062991 N	165.4176222 W	AA1-G14_2	3
64.5063353 N	165.4176265 W	AA1-G14_3	3
64.5062342 N	165.4175867 W	AA1-G14_5	4
64.5062089 N	165.4177000 W	AA1-G14_6	4
64.5061875 N	165.4175526 W	AA1-G14_7	4
64.5063041 N	165.4179330 W	AA1-G14_8	3
64.5063440 N	165.4177745 W	AA1-G14_10	3

AA2 Anomaly Locations and Depths

Latitude	Longitude	Name	Depth
64.5050700 N	165.4169408 W	AA2-G1_1	2
64.5050608 N	165.4172342 W	AA2-G1_3	2
64.5049469 N	165.4173403 W	AA2-G1_4	2
64.5050465 N	165.4170587 W	AA2-G1_5	2
64.5049978 N	165.4171479 W	AA2-G1_6	2
64.5051165 N	165.4169579 W	AA2-G1_7	3
64.5051247 N	165.4170180 W	AA2-G1_8	3
64.5051249 N	165.4171768 W	AA2-G1_9	3
64.5051561 N	165.4170948 W	AA2-G1_10	3
64.5050049 N	165.4173681 W	AA2-G1_12	3
64.5050224 N	165.4169101 W	AA2-G1_14	4
64.5050495 N	165.4171232 W	AA2-G1_15	4
64.5049664 N	165.4173076 W	AA2-G1_17	5
64.5049488 N	165.4171201 W	AA2-G1_18	5
64.5049846 N	165.4170338 W	AA2-G1_19	5
64.5049849 N	165.4173753 W	AA2-G1_20	6
64.5049610 N	165.4173720 W	AA2-G1_21	6
64.5049019 N	165.4170565 W	AA2-G1_22	6
64.5050636 N	165.4171593 W	AA2-G1_24	6
64.5050158 N	165.4171916 W	AA2-G1_25	6
64.5049522 N	165.4175210 W	AA2-G2_1	3
64.5048439 N	165.4176844 W	AA2-G2_2	3
64.5048644 N	165.4176973 W	AA2-G2_3	3
64.5048196 N	165.4175128 W	AA2-G2_4	3
64.5049024 N	165.4173978 W	AA2-G2_6	4
64.5048105 N	165.4176814 W	AA2-G2_7	4
64.5047975 N	165.4175074 W	AA2-G2_9	4
64.5048257 N	165.4176554 W	AA2-G2_10	4
64.5048141 N	165.4175565 W	AA2-G2_11	4
64.5047377 N	165.4175353 W	AA2-G2_12	4
64.5047365 N	165.4175728 W	AA2-G2_13	5
64.5048893 N	165.4174401 W	AA2-G2_14	5
64.5048985 N	165.4172389 W	AA2-G2_15	5
64.5047706 N	165.4173120 W	AA2-G2_16	5
64.5047462 N	165.4173766 W	AA2-G2_17	5
64.5048752 N	165.4176674 W	AA2-G2_18	6
64.5050306 N	165.4178755 W	AA2-G3_2	2
64.5050455 N	165.4176591 W	AA2-G3_4	2
64.5050276 N	165.4176719 W	AA2-G3_5	2
64.5050054 N	165.4176954 W	AA2-G3_6	2
64.5049997 N	165.4177357 W	AA2-G3_7	2
64.5049519 N	165.4177755 W	AA2-G3_8	2
64.5050620 N	165.4178260 W	AA2-G3_10	2
64.5049203 N	165.4175012 W	AA2-G3_11	2
64.5050054 N	165.4175299 W	AA2-G3_12	3
64.5049833 N	165.4175296 W	AA2-G3_13	3
64.5049473 N	165.4175909 W	AA2-G3_15	3
64.5049397 N	165.4177301 W	AA2-G3_16	3
64.5049197 N	165.4177309 W	AA2-G3_17	3

64.5048556 N	165.4178871 W	AA2-G3_20	4
64.5048698 N	165.4177766 W	AA2-G3_22	4
64.5050146 N	165.4178824 W	AA2-G3_23	4
64.5048699 N	165.4179313 W	AA2-G3_24	4
64.5048792 N	165.4178922 W	AA2-G3_25	4
64.5048764 N	165.4178029 W	AA2-G3_27	4
64.5049121 N	165.4176701 W	AA2-G3_29	5
64.5049476 N	165.4176314 W	AA2-G3_30	5
64.5049547 N	165.4176755 W	AA2-G3_31	5
64.5049158 N	165.4178428 W	AA2-G3_32	5
64.5050137 N	165.4176693 W	AA2-G3_36	5
64.5048433 N	165.4178386 W	AA2-G3_38	4
64.5051211 N	165.4175607 W	AA2-G4_2	2
64.5051000 N	165.4174055 W	AA2-G4_3	2
64.5050675 N	165.4173306 W	AA2-G4_5	2
64.5051630 N	165.4173427 W	AA2-G4_6	2
64.5051478 N	165.4173668 W	AA2-G4_7	2
64.5050804 N	165.4173764 W	AA2-G4_8	2
64.5052395 N	165.4175655 W	AA2-G4_9	2
64.5051608 N	165.4171924 W	AA2-G4_10	3
64.5051526 N	165.4173137 W	AA2-G4_12	3
64.5052044 N	165.4172508 W	AA2-G4_14	5
64.5051742 N	165.4173171 W	AA2-G4_15	5
64.5050339 N	165.4174136 W	AA2-G4_16	5
64.5050566 N	165.4174747 W	AA2-G4_17	5
64.5052555 N	165.4174793 W	AA2-G4_18	2
64.5051643 N	165.4174454 W	AA2-G4_19	4
64.5052203 N	165.4173723 W	AA2-G4_20	4
64.5052176 N	165.4174589 W	AA2-G4_21	3
64.5053084 N	165.4171514 W	AA2-G5_1	2
64.5053076 N	165.4174330 W	AA2-G5_2	2
64.5051923 N	165.4170775 W	AA2-G5_3	2
64.5052749 N	165.4172952 W	AA2-G5_4	3
64.5053957 N	165.4173052 W	AA2-G5_5	3
64.5052994 N	165.4169593 W	AA2-G5_6	3
64.5053579 N	165.4171941 W	AA2-G5_7	4
64.5052015 N	165.4170125 W	AA2-G5_9	4
64.5053824 N	165.4172410 W	AA2-G5_10	5
64.5052537 N	165.4169923 W	AA2-G5_11	3
64.5052732 N	165.4169915 W	AA2-G5_12	3
64.5052490 N	165.4170691 W	AA2-G5_13	3
64.5053168 N	165.4170282 W	AA2-G5_14	2
64.5052870 N	165.4170871 W	AA2-G5_15	2
64.5053338 N	165.4173776 W	AA2-G5_16	5
64.5053470 N	165.4169489 W	AA1-G6_1	3
64.5053415 N	165.4169033 W	AA1-G6_2	3
64.5053166 N	165.4169631 W	AA1-G6_3	3
64.5054289 N	165.4168870 W	AA1-G6_4	3
64.5054096 N	165.4172113 W	AA1-G6_5	3
64.5054710 N	165.4169904 W	AA1-G6_6	3

64.5054107 N	165.4172731 W	AA1-G6_7	4
64.5054150 N	165.4170807 W	AA1-G6_8	4
64.5054600 N	165.4170579 W	AA1-G6_9	4
64.5054564 N	165.4172253 W	AA1-G6_10	4
64.5054742 N	165.4171859 W	AA1-G6_11	4
64.5053806 N	165.4171771 W	AA1-G6_12	4
64.5053877 N	165.4168996 W	AA1-G6_13	4
64.5053751 N	165.4168788 W	AA1-G6_14	4

AA2 Anomaly Locations and Depths

Latitude	Longitude	Name	Depth
64.5049880 N	165.4185347 W	AA3-G1_2	3
64.5049316 N	165.4184092 W	AA3-G1_4	3
64.5049687 N	165.4184169 W	AA3-G1_5	3
64.5049820 N	165.4183462 W	AA3-G1_6	4
64.5049506 N	165.4184663 W	AA3-G1_7	6
64.5051248 N	165.4181803 W	AA3-G2_1	2
64.5050429 N	165.4182222 W	AA3-G2_2	2
64.5051563 N	165.4181952 W	AA3-G2_3	2
64.5050056 N	165.4182647 W	AA3-G2_4	2
64.5050731 N	165.4180587 W	AA3-G2_5	2
64.5051317 N	165.4183544 W	AA3-G2_6	3
64.5050384 N	165.4182710 W	AA3-G2_7	3
64.5050914 N	165.4183538 W	AA3-G2_8	3
64.5050864 N	165.4181567 W	AA3-G2_9	4
64.5051488 N	165.4180210 W	AA3-G2_11	4
64.5050527 N	165.4180181 W	AA3-G2_12	4
64.5050601 N	165.4182713 W	AA3-G2_13	5
64.5050297 N	165.4180580 W	AA3-G2_14	5
64.5052218 N	165.4181829 W	AA3-G3_1	2
64.5051823 N	165.4180134 W	AA3-G3_25	5

AA4 Anomaly Locations and Depths

Latitude	Longitude	Name	Depth
64.5048375 N	165.4193891 W	AA4_1	2
64.5049304 N	165.4192292 W	AA4_2	2
64.5049526 N	165.4192424 W	AA4_3	2
64.5049446 N	165.4191358 W	AA4_4	2
64.5047524 N	165.4194782 W	AA4_6	2
64.5049286 N	165.4191243 W	AA4_8	3
64.5048726 N	165.4192509 W	AA4_11	4
64.5048006 N	165.4193772 W	AA4_13	4
64.5048456 N	165.4192150 W	AA4_14	4
64.5049181 N	165.4191644 W	AA4_15	4
64.5048115 N	165.4192290 W	AA4_16	5
64.5048961 N	165.4193125 W	AA4_17	5
64.5048351 N	165.4192438 W	AA4_18	6
64.5047960 N	165.4192933 W	AA4_19	6
64.5050405 N	165.4191324 W	AA4_20	6